Journal of Anatomy

J. Anat. (2018) **233**, pp687–695 doi: 10.1111/joa.12890

Skeletal malformations of Meox1-deficient zebrafish resemble human Klippel–Feil syndrome

Mervyn V. P. Dauer,[1,2] Peter D. Currie[1,2] and Joachim Berger[1,2]

[1]*Australian Regenerative Medicine Institute, Monash University, Clayton, VIC, Australia*
[2]*Victoria Node, EMBL Australia, Clayton, VIC, Australia*

Abstract

Klippel–Feil syndrome is a congenital vertebral anomaly, which is characterised by the fusion of at least two cervical vertebrae and a clinically broad set of symptoms, including congenital scoliosis and elevated scapula (Sprengel's deformity). Klippel–Feil syndrome is associated with mutations in *MEOX1*. The zebrafish mutant *choker* (*cho*) carries a mutation in its orthologue, *meox1*. Although zebrafish is being increasingly employed as fidelitous models of human spinal disease, the vertebral column of Meox1-deficient fish has not been assessed for defects. Here, we describe the skeletal defects of *meox1*^{cho} mutant zebrafish utilising alizarin red to stain bones and chemical maceration of soft tissue to detect fusions in an unbiased manner. Obtained data reveal that *meox1*^{cho} mutants feature aspects of a number of described symptoms of patients who suffer from Klippel–Feil syndrome and have mutations in *MEOX1*. These include vertebral fusion, congenital scoliosis and an asymmetry of the pectoral girdle, which resembles Sprengel's deformity. Thus, the *meox1*^{cho} mutant zebrafish may serve as a useful tool to study the pathogenesis of the symptoms associated with Klippel–Feil syndrome.

Key words: disease modelling; Klippel–Feil syndrome; *MEOX1*; mesenchyme homeobox 1; spinal disease; zebrafish.

Introduction

Klippel–Feil syndrome is a congenital vertebral anomaly, which is diagnosed by the fusion of at least two cervical vertebrae (Klippel & Feil, 1912). Clinically, there is a broad spectrum of symptoms including Sprengel's deformity (congenitally elevated scapula), congenital scoliosis, kyphosis and a range of visceral defects. Klippel–Feil syndrome is reported in 1 : 40 000 live births; however, this is likely to be lower than the actual incidence, as the manifestation of Klippel–Feil syndrome is broad, such that disease severity ranges from seemingly asymptomatic to requiring surgical intervention (Tracy et al. 2004; Krakow, 2018). As there currently is no cure, treatment is focused on symptoms, which are managed through either surgical or lifestyle interventions (Krakow, 2018). Reflecting its clinical heterogeneity, mutations in different genes have been associated with Klippel–Feil syndrome, including *MEOX1*, *GDF3/6*, *RIPPLY2* and *PAX1* (McGaughran et al. 2003; Tassabehji et al. 2008; Ye et al. 2010; Mohamed et al. 2013; Karaca et al. 2015).

Correspondence
Joachim Berger, Peter D. Currie, Australian Regenerative Medicine Institute, Monash University, Clayton, VIC 3800, Australia.
E: Joachim.Berger@monash.edu; Peter.Currie@monash.edu

Accepted for publication *23 August 2018*
Article published online *2 October 2018*

© 2018 Anatomical Society

MEOX1 encodes mesenchyme homeobox 1, a transcription factor expressed in somites and known to be involved in the development of vertebral elements (Candia et al. 1992; Candia & Wright, 1996; Rodrigo et al. 2004; Skuntz et al. 2009; Nguyen et al. 2014). In addition to its DNA-binding homeobox domain, the murine Meox1 orthologue has also been shown to directly bind Pax1 *in vitro* (Stamataki et al. 2001). Furthermore, it has been demonstrated that Meox1 together with Pax1 and Pax9 directly regulate Nkx3-2, which impacts on axial skeleton development (Lettice et al. 1999; Rodrigo et al. 2004; Skuntz et al. 2009). In addition, the zebrafish orthologue, Meox1, is known to directly inhibit the cell cycle regulator Ccnb1 (Nguyen et al. 2017). Despite the clinical heterogeneity of Klippel–Feil syndrome, patients who harbour mutations in *MEOX1* have a set of common reported symptoms. These common symptoms include congenital scoliosis, Sprengel's deformity and the presence of an ectopic omovertebral bone, which connects the scapula with a vertebra (Bayrakli et al. 2013; Mohamed et al. 2013).

Meox1-deficient mice share cervical vertebral fusions with human Klippel–Feil syndrome patients, who harbour mutations in *MEOX1* (Skuntz et al. 2009). However, in contrast to human patients, *Meox1* loss-of-function mice neither develop pectoral girdle asymmetry nor exhibit congenital scoliosis (Skuntz et al. 2009; Bayrakli et al. 2013; Mohamed et al. 2013). In addition, meox1-deficient mice occasionally

feature malsegmentation defects in more posterior regions of the spine, not reported in humans. Zebrafish (*Danio rerio*) has become a popular model system due to their genetic tractability, ex utero development and amenability to microscopy (Lieschke & Currie, 2007). Furthermore, zebrafish are increasingly employed to model human spinal diseases with a high degree of fidelity (Boswell & Ciruna, 2017). The zebrafish mutant *choker* (*cho*) carries a loss-of-function mutation in its orthologue of *MEOX1*, *meox1* (Nguyen et al. 2014). *meox1*^{cho} zebrafish have been previously shown to have somite defects in the posterior hindbrain region and various stem cell defects (van Eeden et al. 1996; Kelsh et al. 1996; Nguyen et al. 2014, 2017). Here, we describe bone defects of *meox1*^{cho} mutants using alizarin red to stain bone and assess the suitability of *meox1*^{cho} zebrafish as a disease model of Klippel–Feil syndrome. We characterise distinct bone defects in *meox1*^{cho} zebrafish, including vertebral fusion, congenital scoliosis and an asymmetry of the pectoral girdle, suggesting that Meox1-deficient zebrafish might be used to model Klippel–Feil syndrome.

Materials and methods

Animal husbandry

The *meox1*^{cho} (*choker*) line was used in the Tübingen genetic background for all experiments (van Eeden et al. 1996; Kelsh et al. 1996). Genotyping for the *meox1*^{cho} allele was performed as described (Nguyen et al. 2014). All zebrafish used were bred and raised as approved by MARP 2017/240.

Alizarin red staining

For whole-mount preparations, adult zebrafish were killed in tricaine and staged by standard length prior to fixation in 4% paraformaldehyde (w/v) for 8–72 h, where fixation duration depended upon specimen size. Adult zebrafish were descaled, skinned and eviscerated before fixation. Larval zebrafish were fixed in ethanol for 4 h to overnight. Samples fixed in paraformaldehyde were dehydrated first in a solution containing 1 part ethanol to 1 part phosphate-buffered saline for 4 h to overnight, followed by ethanol for 4 h to overnight. After dehydration or ethanol fixation, samples were degreased in acetone for a period similar to their fixation period. Subsequently, samples were stained with alizarin red S, bleached and then macerated following established methodology.

To obtain individual and digested adult bones, adults were descaled, skinned and eviscerated prior to fixation in ethanol. Samples were then directly transferred from the fixative to the staining solution. Thereafter, soft tissues were completely macerated in 1% KOH (w/v) at 37 °C, yielding individual bones. The bones were briefly rinsed in water immediately prior to imaging.

Macrophotography

Whole-mount adult zebrafish were photographed using a NEX-5 camera equipped with an E 18–55 mm f/3.5–5.6 OSS objective (Sony). Samples were illuminated with a lightbox. Photographs were subsequently processed in Darktable (v. 2.2.5) software.

Fluorescence microscopy

Dissected pectoral girdles dissected from adult whole-mount alizarin red S-stained preparations were imaged using an MVX10 stereomicroscope equipped with an DP72 camera, MV PLAPO 1 × objective and an RFP filter (Olympus). All images were processed using the GNU Image Manipulation Programme (v. 2.9.6) and Darktable (v. 2.2.5).

Optical slices of whole-mount larval preparations and dissected bones were obtained using an ImagerZ1 microscope with ApoTome and AxioCam HRm camera (Zeiss). A combination of 5 ×, 10 × and 20 × dry objectives with a Texas Red filter cube were used. Maximum intensity and sum slices Z-projections were obtained using Fiji Is Just ImageJ. Where necessary, image tiles were combined using Hugin (v. 2017.0). Images were further processed using the GNU Image Manipulation Programme (v. 2.9.6) and Darktable (v. 2.2.5).

Results

The majority of adult *meox1*^{cho} homozygotes exhibit scoliosis

Externally visible manifestations of spinal malformation were not observed in live adult sibling zebrafish. In contrast, scoliosis occurred in two-thirds of adult *meox1*^{cho} homozygotes across two independent clutches (Fig. S1; clutch 1: n = 20/30; clutch 2: n = 14/22). Thus, a lack of Meox1 is associated with the development of scoliosis in adult zebrafish.

Adult *meox1*^{cho} zebrafish feature fused vertebrae

To visualise bones of adult *meox1*^{cho} homozygotes and siblings, whole-mount alizarin red staining was performed. Although two-thirds of adult *meox1*^{cho} homozygous zebrafish develop externally discernible congenital scoliosis, all examined homozygotes exhibited bone defects in the axial skeleton. Bone defects in *meox1*^{cho} homozygotes were largely confined to the anterior axial skeleton. The exoccipital bone, which is readily distinguishable in siblings on account of the exoccipital foramen (Fig. 1A′, arrowhead; n = 6/6), was reduced in all analysed *meox1*^{cho} mutants (Fig. 1B′, arrowhead; n = 6/6). In siblings, neural arches appeared as long, slender, dorsoposterior projections from centra (Fig. 1A′; n = 6/6); however, in *meox1*^{cho} mutants, the neural arches assumed an altered morphology, where neural arches were anteroposteriorly broadened and dorsoventrally shortened in comparison to their siblings (Fig. 1B′; n = 6/6). In *meox1*^{cho} mutant zebrafish, vertebral fusions were observed between variable vertebrae at the anterior end of the vertebral column between neural arches (Fig. 1B′, arrowheads; n = 6/6).

To further assess whether these defects are *bona fide* fusions, whole, alizarin red-stained adult fish were

© 2018 Anatomical Society

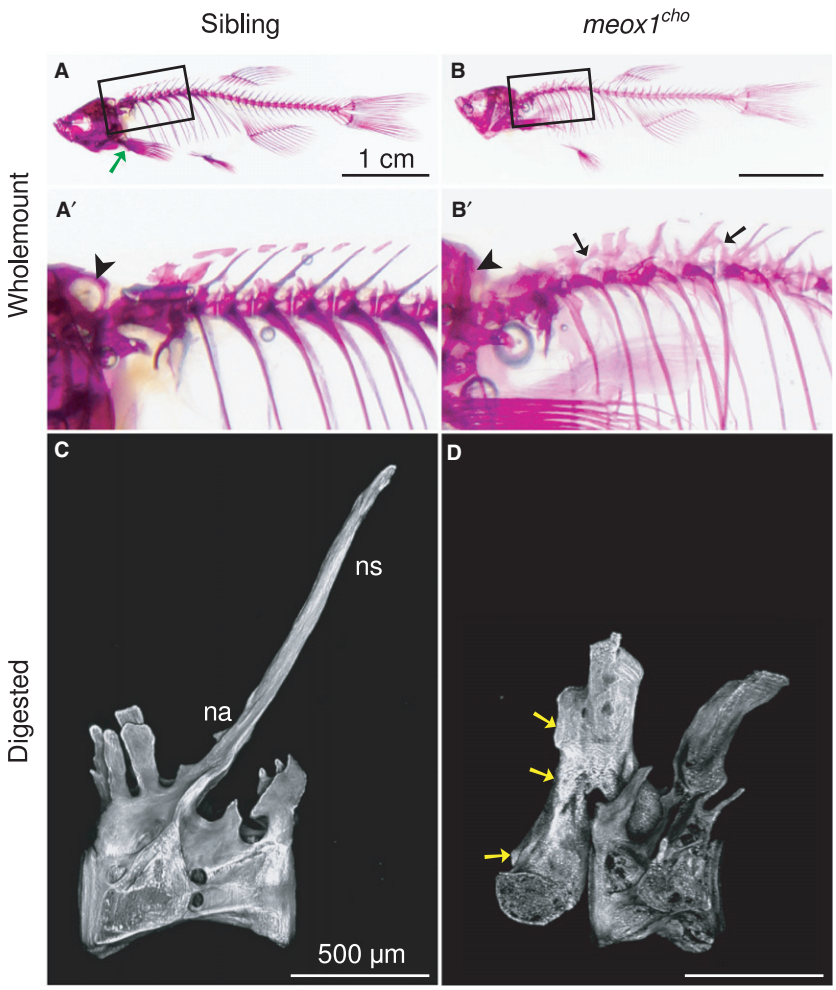

Fig. 1 Bone defects coalesce anteriorly in *meox1*^{cho} mutant zebrafish. (A,B) Lateral views of whole-mount alizarin red-stained 32-mm standard length adult siblings and homozygotes reveal that bone defects within *meox1*^{cho} homozygotes are confined to the axial skeleton. The boxed regions are magnified in (A′) and (B′). A green arrow indicates the location of the pectoral girdle. (A′,B′) The exoccipital foramen is readily discerned in siblings (A′, arrowhead, $n = 6/6$) and is not evident in whole-mount *meox1*^{cho} homozygous mutants (B′, arrowhead, $n = 6/6$). Vertebral fusion is evident in vertebræ across neural arches (B′, arrows, $n = 6/6$). (C) Lateral maximum intensity Z-projection of a chemically isolated vertebra shows the morphology typical of a vertebra from the anterior region of the wild-type zebrafish spine. (D) Lateral view of a chemically isolated vertebra involved in an apparent anterior fusion in a *meox1*^{cho} adult mutant. Fusion occurred between neural arches (arrows); however, only one vertebral centrum was incorporated. na, neural arch; ns, neural spine. Scale bars: 1 cm (A,B); 500 µm (C,D).

subjected to total chemical digestion. This allowed for the removal of all soft tissues leaving only mineral bone remaining. Complete digestion of soft tissues confirmed the anterior fusions observed in whole-mount preparations. Furthermore, these vertebral fusions were partial, i.e. a single vertebra was fused to its own neural arches in addition to that of its neighbouring vertebra (Fig. 1D, arrows).

Vertebrae 1–4 in the zebrafish comprise the Weberian vertebrae, which are distinguishable by specialised modifications and form part of the Weberian apparatus. The Weberian apparatus enables the transduction of vibrations from the swimbladder to the fish's inner ear. In neither *meox1*^{cho} homozygotes nor siblings were these vertebrae readily discernible in whole-mount preparations due to the highly specialised and spatially overlapping Weberian ossicles surrounding the vertebral centra. However, chemical digestion of soft tissues enabled the isolation of these fragile and deep bones with minimal handling. In all siblings, the Weberian neural arches of vertebrae 3 and 4 did not form a contiguous bony element; rather, they were conterminous and separable by maceration of connective soft tissues (Fig. 2A–E). In homozygous *meox1*^{cho} mutant zebrafish, the corresponding centra and its neural arches were observed to be fused as a single bony unit (Fig. 2F, dotted line). Occasionally, fused elements consisted of a centrum, its neural arches and a neural arch of its immediate neighbour (Fig. 2G), or these elements were completely fused and consisted of two centra and their neural arches (Fig. 2H). Where vertebral fusion did occur, synostoses were between neural arches and not between

© 2018 Anatomical Society

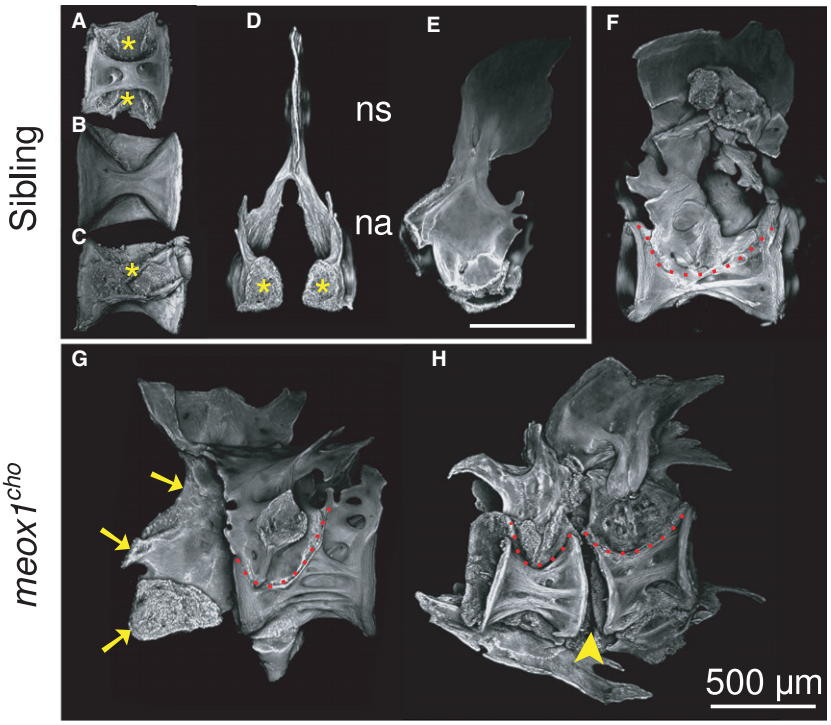

Fig. 2 The anterior-most vertebral elements in *meox1*^{cho} mutants have fusions within and across vertebrae. (A–E) Maximum intensity Z-projections of Weberian centra (respectively, dorsal, ventral and lateral views) and neural arches (respectively, medioanterior and lateral views) isolated from siblings reveal that centra and neural arches are discrete and conterminous bony elements within the Weberian apparatus. Articular surfaces are apparent (asterisks). (F–H) In *meox1*^{cho} homozygotes, neural arches are fused to centra (dotted lines), excepting where a centrum has fused to its arches and an arch of its neighbour (G, arrows). Where fusion incorporated two centra into a single bony element, the intervertebral gap was discernible (arrowheads). (F–H) Lateral views, where anterior is left. na, neural arch; ns, neural spine. Scale bars: 500 µm.

centra, as the intervertebral space remained perceptible (Fig. 2H, arrowhead).

In addition to fusions in anterior regions of the *meox1*^{cho} mutant vertebral column, fusions were sporadically detected throughout the entirety of mutant spines following digestion (Fig. 3B,D). Excluding the specialised Weberian vertebrae, all precaudal and caudal vertebrae in digested sibling preparations were discrete bony elements broadly comprising of a centrum, neural arches and haemal arches (Fig. 3A,C). In digests of *meox1*^{cho} mutant zebrafish, fused vertebrae were sporadically present in all regions of the spine, where fusion was between either neural (Fig. 3D, arrows) or haemal arches (Fig. 3B,B′, arrow). Similar to fusions of more anterior vertebrae, an intervertebral space was detectable (Fig. 3B,D,D′, arrowheads). Thus, vertebral fusions in *meox1*^{cho} mutants were confined between vertebral arches.

Meox1 is involved in neural arch fusion at the midline

Excepting the distinct Weberian vertebrae, adult zebrafish vertebrae comprise broadly of a centrum, neural arches, a neural spine and, where applicable, haemal arches and a haemal spine; Fig. 4A,B,E,F). In contrast to siblings, the vertebrae of *meox1*^{cho} mutants, which are not involved in a vertebral fusion, comprise these same elements. However, in the case of more posterior precaudal and caudal vertebrae, the neural arches and occasionally the haemal arches fail to join at the midline and project two spines, one for each arch (Fig. 4C,D,G,H, arrowheads, boxes). Moreover, the right neural arch was observed to be shorter and projected less posteriorly than left neural arches (Fig. 4C′,D′,G′, H′), indicating that Meox1 is involved in neural arch fusion at the midline.

meox1^{cho} mutant zebrafish have pectoral asymmetry

Patients suffering from Klippel–Feil syndrome are often diagnosed with Sprengel's deformity, where one scapula is elevated relative to the other. Given the asymmetry in *meox1*^{cho} mutant neural arches described above and that patients with Klippel–Feil syndrome with mutations in *MEOX1* have the asymmetry that is Sprengel's deformity (Bayrakli et al. 2013; Mohamed et al. 2013), the pectoral girdle was assessed. Despite the anatomical differences between fish and human pectoral girdle architecture, such as the presence of a cleithra in zebrafish but not humans, we find that in the dissected pectoral girdles of *meox1*^{cho}

© 2018 Anatomical Society

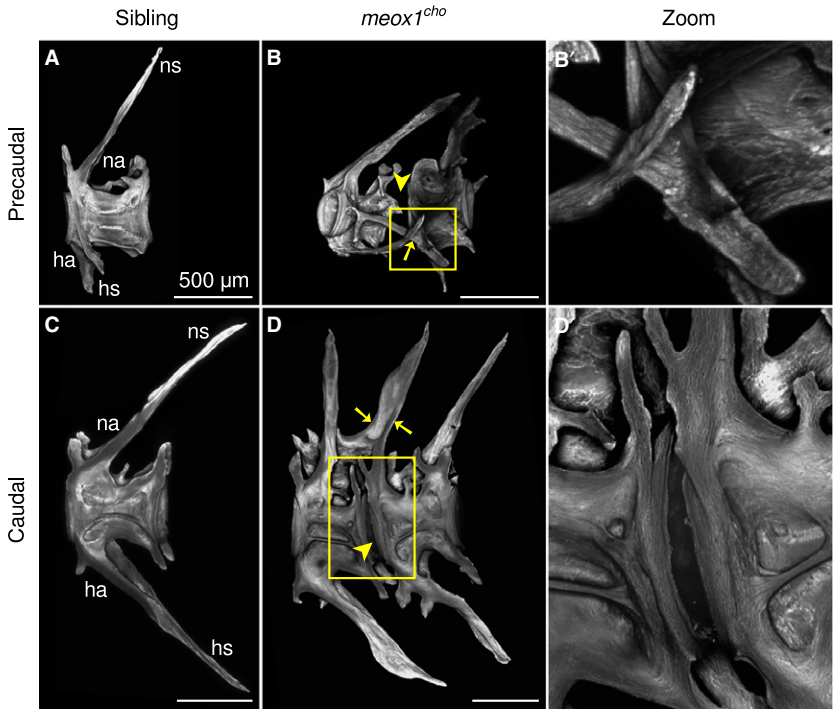

Fig. 3 Adult *meox1*^{cho} zebrafish have fused precaudal and caudal vertebrae. (A,C) Maximum intensity Z-projections of chemically isolated precaudal (A) and caudal (C) sibling vertebrae. (B,D) In *meox1*^{cho} homozygotes, vertebral fusion occurs between haemal (B, arrow) and neural (D, arrows) arches; however, the intervertebral space between centra remains appreciable (arrowheads). Boxed regions are magnified in (B′) and (D′). (B′) The right haemal arch of the more anterior vertebra has extended more leftward than the right haemal arch, which has fused to the right haemal arch of the neighbouring vertebra. (D′) A magnified view of the intervertebral region shows that the vertebral centra are discrete despite their proximity in *meox1*^{cho} homozygotes. All panels are lateral views, where anterior is left. ha, haemal arch; hs, haemal spine; na, neural arch; ns, neural spine. Scale bars: 500 µm.

homozygotes, the left side was observed to be more anterior than the right (Fig. 5B; $n = 3/3$). Those of sibling zebrafish were symmetrical (Fig. 5A; $n = 3/3$). In all analysed fish, it was noted that the left postcleithra of mutant pectoral girdles had projected anteriorly, whereas the right postcleitha were unremarkable (Fig. 5B, arrow). Thus, *meox1*^{cho} mutant zebrafish feature defects similar to the human Sprengel's deformity.

Vertebral fusions within *meox1*^{cho} larvae occur at the onset of vertebral development

In zebrafish, the onset of vertebral formation is initiated at 4.6 mm standard length, where vertebral centra arise as direct ossifications of the notochord (Bird & Mabee, 2003; Inohaya et al. 2007). To assess defects at the onset of vertebral development, the early larval centra of both siblings and *meox1*^{cho} homozygotes were subjected to whole-mount alizarin red staining (Fig. 6). At 4.6–4.9 mm standard length, centra of sibling zebrafish were discrete with well-defined borders (Fig. 6A; $n = 4/4$), whereas fusions were observed in *meox1*^{cho} homozygotes variably between vertebrae 1–4 (Fig. 6B, arrows; $n = 4/5$). At earlier stages, all centra are discrete in *meox1*^{cho} larvae and are unaffected upon comparison with their siblings (data not shown). All larval centra posterior to vertebra 4 were unremarkable in analysed *meox1*^{cho} mutant larvae in comparison to their siblings of similar standard length (data not shown). In conclusion, Meox1 is involved in the early segmentation of the anterior vertebrae.

Discussion

Given the differences between the proclivities of bipedal humans and quadrupedal animals to the development of spinal disease, the use of some popular model organisms, such as mice, to fideliously model human spinal diseases may prove challenging. For example, *Meox1*$^{-/-}$ mice share only anterior axial synostoses with human Klippel–Feil syndrome patients, who have mutations in *MEOX1* (Skuntz et al. 2009; Bayrakli et al. 2013; Mohamed et al. 2013). Despite their lack of a load-bearing spinal column and being more phylogenically removed from humans than mice, fish such as zebrafish are frequently used to model human spinal disease (Gorman & Breden, 2007; Boswell & Ciruna, 2017).

The hallmark of Klippel–Feil syndrome is the fusion of cervical vertebrae. Cervical vertebrae are unique to tetrapods

© 2018 Anatomical Society

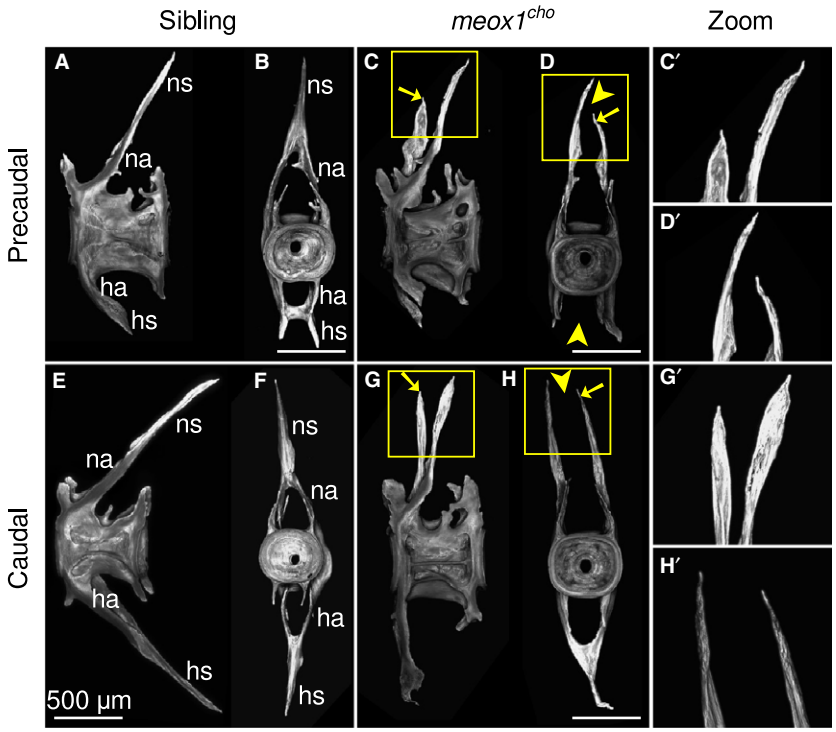

Fig. 4 Neural arches in *meox1*^{cho} mutants are typically unfused at the midline and are asymmetric. (A,B,E,F) Maximum intensity Z-projections of precaudal and caudal vertebrae both laterally (A,E) and posteriorly (B,F) show that vertebrae are symmetric, and that vertebral arches fuse at the midline and project a single neural or haemal spine. (C,D,G,H) Exemplar precaudal and caudal vertebrae of an adult *meox1*^{cho} mutant viewed both laterally (C,C′,G,G′) and posteriorly (D,D′,H,H′) show that the neural arches and occasionally the haemal arch is unfused at the midline (arrowheads). The left neural arch is more anterior and shorter than the right (arrows). (C′,D′,G′,H′) Magnified views of the boxed regions in (C,D,G,H). ha, haemal arch; hs, haemal spine; na, neural arch; ns, neural spine. Scale bars: 500 µm.

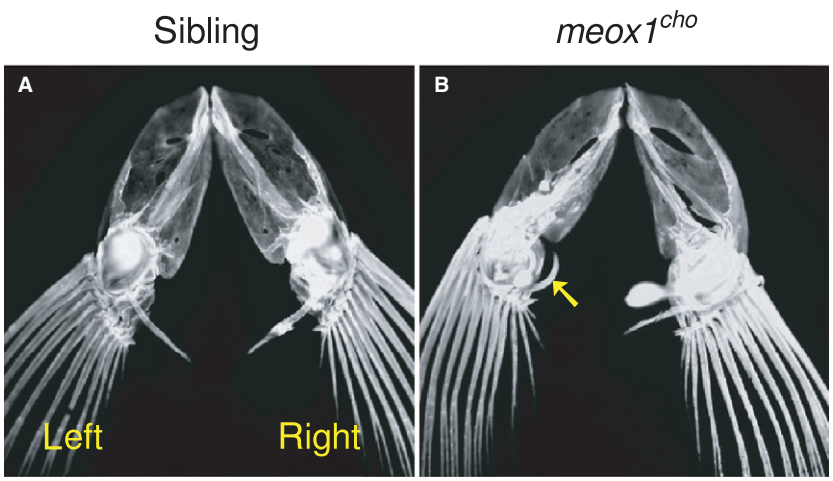

Fig. 5 The pectoral girdle of *meox1*^{cho} mutant zebrafish is more anterior on the left than the right. (A) A dorsal view of pectoral girdles of cleared, alizarin red-stained sibling zebrafish shows that they are symmetrical ($n = 3/3$). (B) In *meox1*^{cho} homozygotes, the left side is more anterior than the right ($n = 3/3$). The left postcleithrum has extended anteriorly (arrowhead).

and are not present in fish. Nonetheless, *meox1*^{cho} mutant zebrafish maintain skeletal defects in an equivalent anterior region immediately posterior to the cranium at both larval and adult stages of life. Human Klippel–Feil syndrome patients with mutations in *MEOX1* have deformities in the occipital bone, such that the occipital bone is fused to parts of the atlas and axis, or is deformed (Bayrakli et al. 2013; Mohamed et al. 2013). Therefore, the synostoses associated with Klippel–Feil syndrome are not confined to cervical vertebrae; rather, they are confined to an anterior region that

© 2018 Anatomical Society

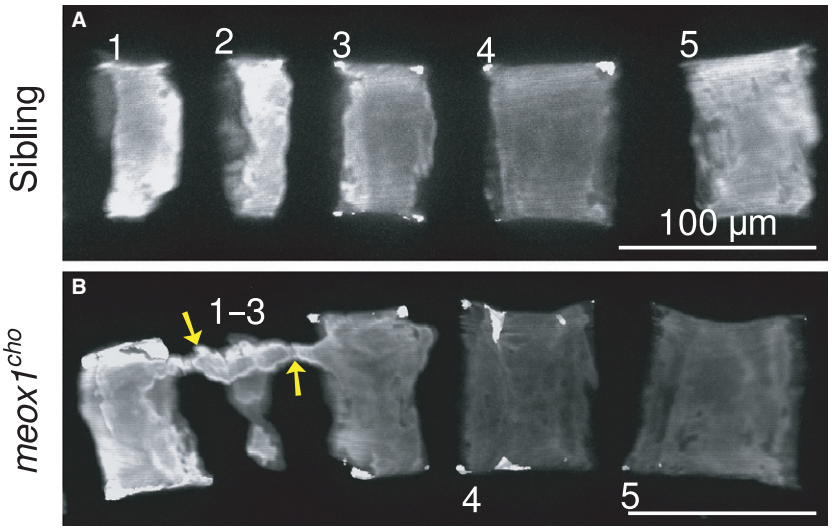

Fig. 6 Vertebral fusion is observed shortly after the formation of the anterior-most vertebrae. (A) Lateral maximum intensity Z-projection of the anterior-most vertebrae of a 4.6–4.9-mm standard length larval sibling reveals that centra are discrete and well defined ($n = 4/4$). (B) Fusion between vertebrae 1–3 is evident as a bony bridge spanning the dorsum of developing centra in this 4.6–4.9-mm standard length *meox1*^{cho} mutant (arrows). Fusions were variably observed between vertebrae 1–4 in mutants of the same standard length ($n = 4/5$). Numbers indicate vertebrae. Scale bars: 100 μm.

includes the cervical vertebrae and posterior occipital bones in humans. In agreement with patient observations, the exoccipital bone in *meox1*^{cho} mutant zebrafish was also misshapen. Similar in *Meox1*$^{-/-}$ mice, synostoses affect both occipital bones and cervical vertebrae (Skuntz et al. 2009). These across-species data suggest that *MEOX1* and its orthologues are involved in patterning an anterior region of the axial skeleton, which includes the anterior-most vertebrae and the posterior exoccipital bones across vertebrates. In addition to occipital defects detected in human patients, *meox1*^{cho} mutant zebrafish have synostoses within and between anterior vertebrae. Therefore, notwithstanding their lack of cervical vertebrae, homozygous *meox1*^{cho} zebrafish feature the characteristic localised fusions associated with Klippel–Feil syndrome.

Although autonomous segmentation of the notochord was suggested as the developmental origin of segmental patterning of centra in teleosts, an influence by the paraxial mesoderm was demonstrated (Lleras-Forero et al. 2018). Interestingly, loss of Meox1 function within the paraxial mesoderm, as seen within *meox1*^{cho} mutants (Nguyen et al. 2014), leads to vertebrae defects. Therefore, the signal from the paraxial mesoderm that influences the segmentation of centra might be disrupted in the absence of Meox1 within the anterior region.

In addition to cervical fusion and congenital scoliosis, patients suffering from Klippel–Feil syndrome are also diagnosed with Sprengel's deformity (congenitally elevated scapula) and ectopic omovertebral bone formation. Adult *meox1*^{cho} homozygotes displayed comparable bone defects, with the exception of an ectopic bony connection between the pectoral girdle and a vertebra. This is striking, as there are a number of anatomical differences between the zebrafish and human pectoral girdle, such as the location of the girdle relative to the axial skeleton and whether dermal bones are present (McGonnell, 2001). However, with the embryological origins of the omovertebral bone being contentious (Matsuoka et al. 2005; Dhir et al. 2018), determination of the structure homologous to the omovertebral bone would be controversial. Klippel–Feil syndrome is noted for its heterogeneity in severity. Accordingly, two-thirds of adult *meox1*^{cho} homozygous zebrafish developed congenital scoliosis. Furthermore, pectoral girdle asymmetry was observed in *meox1*^{cho}, which is reminiscent of Sprengel's deformity. In patients suffering from Sprengel's deformity, the left shoulder is more often affected than the right, with bilateral scapular elevation occurring rarely (Di Gennaro et al. 2012). Zebrafish *meox1*^{cho} mutants are also characterised by a left–right bias in the pectoral girdle, with the left side being positioned more anteriorly than the right. Therefore, *meox1*^{cho} mutants feature aspects of a number of symptoms, which are characteristic of Klippel–Feil syndrome associated with mutations in *MEOX1*. Interestingly, expression of *Nkx3-2*, whose expression is directly regulated by *Meox1*, exhibits transient left–right asymmetry in mice and chick (Schneider et al. 1999). Although the role of *Nkx3-2* in axial skeletal development and chondrogenesis has been demonstrated, the significance of its asymmetric expression is hereunto unknown (Schneider et al. 1999). Therefore, it could be speculated that the aetiology of Sprengel's deformity is associated with developmental dysregulation of *NKX3-2*. A future study could explore what role Meox1 has in left–right patterning using the *meox1*^{cho} mutant zebrafish model.

© 2018 Anatomical Society

Although *meox1*^{cho} zebrafish recapitulate aspects of Klippel–Feil syndrome, these mutant zebrafish conspicuously harbour fusions throughout the vertebral column. Additionally, *meox1*^{cho} homozygotes exhibit a failure of the left and right vertebral arches of precaudal and caudal vertebrae to fuse at the midline, with neural arches being more affected than haemal arches. Within the zebrafish precaudal and caudal vertebrae, the aforementioned vertebral synostoses and failure of fusion are likely different phenotypes arising from the same underlying developmental defect. In *meox1*^{cho} mutants, left and right neural arches fail to fuse and are asymmetric in *meox1*^{cho} mutant zebrafish, such that left arches are more anterior than right arches. Considering this and the thinness of zebrafish vertebral arches, it is likely that fusion has arisen as the result of defective growth of neighbouring arches, such that these arches are within proximity of each other. This is in contrast to the aforementioned anterior fusion, which in *meox1*^{cho} mutants occurs where in zebrafish the neural arches are thickest and likely arose through a differing mechanism, as evidenced by the larval fusion observed in early centra development at this region. A similar neural arch fusion defect has been reported in patients with Klippel–Feil syndrome, where the left and right neural arches of some cervical vertebrae fail to fuse at the midline (Bayrakli et al. 2013). Interestingly, mice deficient for Meox1 occasionally exhibit fusion defects in posterior spinal regions; however, these defects were reported as split centra as opposed to neural arch defects (Skuntz et al. 2009). In both humans and zebrafish lacking *meox1* orthologues, this neural arch fusion defect occurs in the least substantial neural arches within respective vertebral columns. Therefore, although *meox1*^{cho} zebrafish have fusions throughout its vertebral column, this defect remains relevant to modelling Klippel–Feil syndrome.

In summation, *meox1*^{cho} mutant zebrafish feature aspects of a range of symptoms associated with patients suffering from Klippel–Feil syndrome, such as 'cervical' fusion, congenital scoliosis, Sprengel's deformity and neural arch fusion defects. When considering the innate differences in vertebral anatomy between zebrafish and humans, the bone defects that characterise *meox1*^{cho} fish were remarkably comparable to human patients who carry mutations in *MEOX1*. This suggests that the role of *MEOX1* orthologues in patterning vertebral arches and an anterior region of the axial skeleton is highly conserved across species. Thus, *meox1*^{cho} zebrafish are poised to serve as a useful tool to further our understanding of the pathogenesis of Klippel–Feil syndrome and the relatedness of its various symptoms.

Acknowledgements

The authors thank Monash Micro Imaging for technical support. P.D.C. and J.B. were supported by the National Health and Medical Research Council of Australia (APP1144159 and APP1084944 to P.D.C and J.B; APP1136567 to P.D.C.). The Australian Regenerative Medicine Institute is supported by grants from the State Government of Victoria and the Australian Government.

Conflict of interest

The authors declare no conflict of interest.

Author contributions

M.V.P.D. performed the experiments and analysis of data. J.B. and P.D.C. conceived experiments and performed data analysis. All authors wrote and edited the manuscript.

References

Bayrakli F, Guclu B, Yakicier C, et al. (2013) Mutation in *MEOX1* gene causes a recessive Klippel–Feil syndrome subtype. *BMC Genet* **14**, 95.

Bird NC, Mabee PM (2003) Developmental morphology of the axial skeleton of the zebrafish, *Danio rerio* (Ostariophysi: Cyprinidae). *Dev Dyn* **228**, 337–357.

Boswell CW, Ciruna B (2017) Understanding idiopathic scoliosis: a new zebrafish school of thought. *Trends Genet* **33**, 183–196.

Candia AF, Wright C (1996) Differential localization of Mox-1 and Mox-2 proteins indicates distinct roles during development. *Int J Dev Biol* **40**, 1179–1184.

Candia AF, Hu J, Crosby J, et al. (1992) *Mox-1* and *Mox-2* define a novel homeobox gene subfamily and are differentially expressed during early mesodermal patterning in mouse embryos. *Development* **116**, 1123–1136.

Dhir R, Chin K, Lambert S (2018) The congenital undescended scapula syndrome: sprengel and the cleithrum: a case series and hypothesis. *J Shoulder Elbow Surg* **27**, 252–259.

Di Gennaro G, Fosco M, Spina M, et al. (2012) Surgical treatment of Sprengel's shoulder: experience at the Rizzoli Orthopaedic Institute 1975-2010. *J Bone Joint Surg Br* **94**, 709–712.

van Eeden F, Granato M, Schach U, et al. (1996) Mutations affecting somite formation and patterning in the zebrafish, *Danio rerio*. *Development* **123**, 153–164.

Gorman KF, Breden F (2007) Teleosts as models for human vertebral stability and deformity. *Comp Biochem Physiol C Toxicol Pharmacol* **145**, 28–38.

Inohaya K, Takano Y, Kudo A (2007) The teleost intervertebral region acts as a growth center of the centrum: in vivo visualization of osteoblasts and their progenitors in transgenic fish. *Dev Dyn* **236**, 3031–3046.

Karaca E, Yuregir OO, Bozdogan ST, et al. (2015) Rare variants in the notch signaling pathway describe a novel type of autosomal recessive Klippel-Feil syndrome. *Am J Med Genet A* **167**, 2795–2799.

Kelsh R, Brand M, Jiang Y, et al. (1996) Zebrafish pigmentation mutations and the processes of neural crest development. *Development* **123**, 369–389.

Klippel M, Feil A (1912) Un cas d'absence des vertèbres cervicales avec cage thoracique remontant jusqu'à la base du crâne (cage thoracique cervicale). *Nouv Iconog Salpêtrière* **25**, 223–250.

Krakow D (2018) Spinal abnormalities and Klippel–Feil syndrome. In: *Obstetric Imaging: Fetal Diagnosis and Care*. (eds Copel JA, D'Alton ME, Feltovich H, Gratacós E, Krakow D,

© 2018 Anatomical Society

Odibo AO, Platt LD, Tutschek B), pp. 295–297. Philadelphia: Elsevier.

Lettice LA, Purdie LA, Carlson GJ, et al. (1999) The mouse bagpipe gene controls development of axial skeleton, skull, and spleen. *Proc Natl Acad Sci USA* **96**, 9695–9700.

Lieschke GJ, Currie PD (2007) Animal models of human disease: zebrafish swim into view. *Nat Rev Genet* **8**, 353–367.

Lleras-Forero L, Narayanan R, Huitema LFA, et al. (2018) Segmentation of the zebrafish axial skeleton relies on notochord sheath cells and not on the segmentation clock. *ELife* **7**, e33843.

Matsuoka T, Ahlberg PE, Kessaris N, et al. (2005) Neural crest origins of the neck and shoulder. *Nature* **436**, 347.

McGaughran J, Oates A, Donnai D, et al. (2003) Mutations in PAX1 may be associated with Klippel-Feil syndrome. *Eur J Hum Genet* **11**, 468–474.

McGonnell I (2001) The evolution of the pectoral girdle. *J Anat* **199**, 189–194.

Mohamed JY, Faqeih E, Alsiddiky A, et al. (2013) Mutations in MEOX1, encoding mesenchyme homeobox 1, cause Klippel-Feil anomaly. *Am J Hum Genet* **92**, 157–161.

Nguyen PD, Hollway GE, Sonntag C, et al. (2014) Haematopoietic stem cell induction by somite-derived endothelial cells controlled by *meox1*. *Nature* **512**, 314–318.

Nguyen PD, Gurevich DB, Sonntag C, et al. (2017) Muscle stem cells undergo extensive clonal drift during tissue growth via Meox1-mediated induction of G2 cell-cycle arrest. *Cell Stem Cell* **21**, 107–119.

Rodrigo I, Bovolenta P, Mankoo BS, et al. (2004) Meox homeodomain proteins are required for *Bapx1* expression in the sclerotome and activate its transcription by direct binding to its promoter. *Mol Cell Biol* **24**, 2757–2766.

Schneider A, Mijalski T, Schlange T, et al. (1999) The homeobox gene it *NKX3.2* is a target of left–right signalling and is expressed on opposite sides in chick and mouse embryos. *Curr Biol* **9**, 911–914.

Skuntz S, Mankoo B, Nguyen M-TT, et al. (2009) Lack of the mesodermal homeodomain protein MEOX1 disrupts sclerotome polarity and leads to a remodeling of the cranio–cervical joints of the axial skeleton. *Dev Biol* **332**, 383–395.

Stamataki D, Kastrinaki M-C, Mankoo BS, et al. (2001) Homeodomain proteins Mox1 and Mox2 associate with Pax1 and Pax3 transcription factors. *FEBS Lett* **499**, 274–278.

Tassabehji M, Fang ZM, Hilton EN, et al. (2008) Mutations in GDF6 are associated with vertebral segmentation defects in Klippel-Feil syndrome. *Hum Mutat* **29**, 1017–1027.

Tracy M, Dormans J, Kusumi K (2004) Klippel-Feil syndrome: clinical features and current understanding of aetiology. *Clin Orthop Relat Res* **424**, 183–190.

Ye M, Berry-Wynne KM, Asai-Coakwell M, et al. (2010) Mutation of the bone morphogenetic protein *GDF3* causes ocular and skeletal anomalies. *Hum Mol Genet* **19**, 287–298.

Supporting Information

Additional Supporting Information may be found online in the Supporting Information section at the end of the article:

Fig. S1 Scoliosis occurs in two-thirds of *meox1*^{cho} adult homozygotes.

© 2018 Anatomical Society